Low-noise large-bandwidth high-gain transimpedance amplifier for cryogenic STM at 77 K

Ying-Xin Liang[1]*, Ru-Nan Shang[1], Fang-Hao Liang[2], Hao Zhang[3], Ke He[3]
[1]Beijing Academy of Quantum Information Sciences,Haidian, 100193, beijing, China
[2]School of Mathematics, Shandong University, Jinan 250100, Shandong, China
[3]State Key Laboratory of Low Dimensional Quantum Physics,
Department of Physics, Haidian, 100084, beijing, China

April 21, 2024

Abstract

In this work, we design and fabricate the transimpedance Amplifier (TIA) following the design mentioned in Ref.[1]. In the TIA, the preamplifier (Pre-Amp) is made of a junction field effect transistor (JFET) that can work at 77 K. The post-amplifier is made of an operational amplifier (OPA). Cascade Pre-Amp and Post-Amp to form the inverting-amplifier (Inv-Amp). The gain-bandwidth product of Inv-Amp with the gain about 50,000 is higher than 10 GHz. With a 1.13 GΩ feedback network, the gain of TIA is 1.13 GΩ and its bandwidth is about 97 kHz. The equivalent input noise voltage power spectral density of TIA is not more than 9 $(\mathrm{nV})^2/\mathrm{Hz}$ at 10 kHz and 4 $(\mathrm{nV})^2/\mathrm{Hz}$ at 50kHz, and its equivalent input noise current power spectral density is about 26 $(\mathrm{fA})^2/\mathrm{Hz}$ at 10 kHz and 240 $(\mathrm{fA})^2/\mathrm{Hz}$ at 50 kHz. The measured transport performances and noise performances of TIA are consistent with the simulations and calculations, verifying the feasibility for the design of low-noise large-bandwidth TIA proposed in Ref.[1]. And, TIA with various performances that meet various needs can be designed according to the design methods in Ref.Ref.[1, 2]. With the same gain, the bandwidth of the TIA in this work is much larger than the present TIA and its noises are much lower than those of present ones. The TIA in this work is perfect for the cryogenic STM working at 77 K (i.e. liquid nitrogen temperature).

1 Introduction

For cryogenic scanning tunneling microscope (CryoSTM), scanning tunneling spectroscopy (STS) and scanning tunnel shot noise spectroscopy (STSNS) [1, 2] are important means to investigate novel phenomena in quantum systems. High performance transimpedance amplifier (TIA) is a key element in CryoSTM for STS and STSNS measurements. The gain and bandwidth of TIA, as well as its inherent noise, determine its performance in the measurements. For a TIA, the inherent noise is characterized by equivalent input noise voltage and equivalent input noise current. And, the noise parameters are typically equivalent input noise voltage power spectral density (PSD) and equivalent input noise

*cryoliang@qq.com

current PSD. Commercial TIAs for CryoSTM, such as FEMTO DE-DLPC-200 [3], as its gain is 1 GΩ, its bandwidth is only 1 kHz, and its equivalent input noise voltage PSD is 16 $(\mathrm{nV})^2/$ Hz in the frequencies of $f > 100$ Hz, and its equivalent input noise current PSD is 18.5 $(\mathrm{fA})^2/$ Hz at $f = 100$ Hz. In recent years, several designs of TIA in CryoSTM are proposed based on new design ideas [1, 2, 4, 5]. For them, as the gain is 1 GΩ, the bandwidth is larger than 100 kHz. And, the equivalent input noise voltage PSD can be lower than 0.5 $(\mathrm{nV})^2/\mathrm{Hz}$ in $f > 10$ kHz, and the equivalent input noise current PSD is 0.28 $(\mathrm{fA})^2/\mathrm{Hz}$ at $f = 10$ kHz and 5.3 $(\mathrm{fA})^2/\mathrm{Hz}$ at $f = 100$ kHz. With the proposed TIA in CryoSTM, the STS measurements can be performed with the gain of 1 GΩ at the frequency of tens of kHz[1, 2]. However, these designed TIAs have not been fabricated and their performances have not been checked by measurements.

In this work, based on the proposed TIA design methods in Ref.[1], the TIA with the same circuit topology as that in Ref.[1] are fabricated. A junction field effect transistor (JFET) is instead of the expensive CNRS-HEMT[6, 7]. As a cheap demo, the performances of TIA, such as transimpedance gain, bandwidth, and inherent noises etc., are measured at 77 K. The measurement results are consistent with the theoretical calculation results and the simulation results in design, which verifies the feasibility for the design of the proposed TIA in Ref.[1]. As the gain of the JFET-based TIA is 1.13 GΩ, its bandwidth is about 97 kHz. And, its equivalent input noise voltage PSD is about 8 $(\mathrm{nV})^2/\mathrm{Hz}$ at $f = 10$ kHz and 3.7 $(\mathrm{nV})^2/\mathrm{Hz}$ at $f = 50$ kHz, and its equivalent input noise current PSD is about 26$(\mathrm{fA})^2/\mathrm{Hz}$ at $f = 10$ kHz and 240 $(\mathrm{fA})^2/\mathrm{Hz}$ at $f = 50$ kHz. If this TIA is used for CryoSTM operating at 77 K, compared with FEMTO DE-DLPCA-200, the STS measurement with the same accuracy can be performed with 10 times higher speed, and the STSNS measurement can be performed at the frequency of tens of kHz.

2 Circuit of TIA and its amplifing performances

In CryoSTM, TIA is connected to a signal source circuit containing a tunnel junction (TJ) is denoted as TJ-TIA. The TJ-TIA circuit is shown in Fig.1, and the parameters of its components are shown in Table 1. Premplifier (Pre-Amp) is shown in Fig.1(a1) and Fig.1(a2); Post-amplifier (Post-Amp) is shown in Fig.1(b); the feedback network with frequency compensation is shown in Fig.1(c); and the signal source circuit is shown in Fig.1(d). Cascading Pre-Amp and Post-Am form an inverting Amplifier (Inv-Amp). Connecting the feedback network on the Inv-Amp constitutes a TIA. TIA connected signal source circuit is TJ-TIA.

2.1 Pre-Amplifier

Fig.1(a1) shows the of Pre-Amp. In Pre-Amp, the JFET is a N-Channel Depletion-Mode JFET, and SST4393-T1 as JFET is selected in this work [8]. SST4393-T1 can operate at 77K. The parameters of the components in single-transistor amplifier circuit are shown in Table 1. The gate G of JFET is the input of Pre-Amp. O1 and O2 are called the inverting and positive outputs of Pre-Amp respectively, and they are connected to the two inputs of the Post-Amp. JFET, R_{s}, R_{h}, R_1, and R_2 in Pre-Amp are placed in cryogenic zone at 77 K. The capacitance of the cable between the tip of the CryoSTM is C_{I}. The JFET should be placed to the tip of the CryoSTM as close as possible, so that C_{I} is reduced to less than

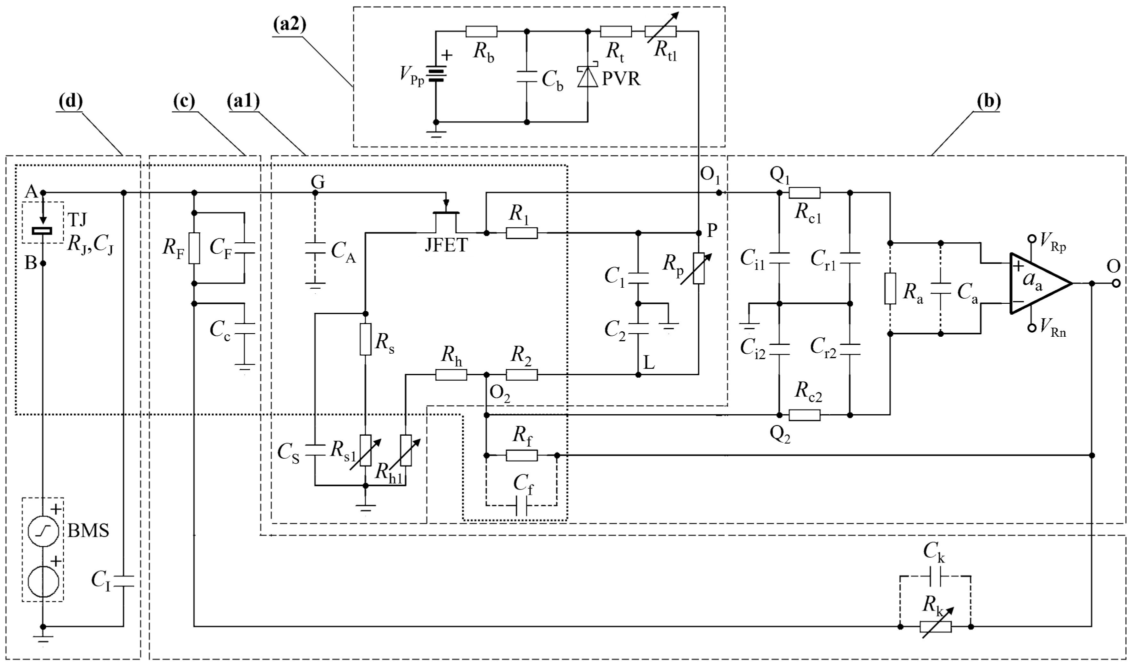

Figure 1: Circuit of the proposed TJ-TIA. Single HEMT amplifier part of Pre-Amp is shown in dashed box (a1), power supply of Pre-Amp in dashed box (a2), Post-Amp in dashed box (b), compensated feedback network in dashed box (c), and signal source circuit in dashed box (d). The components placed in the cryogenic zone are shown in the dotted box. The parameters of all components of CryoSTM-TIA circuit are listed in Table 1.

0.5 pF. Variable resistors R_{s1}, R_{h1}, and R_{p} are placed at room temperature. Fig.1(a2) shows the power supply for Pre-Amp, and the parameters of its components are shown in Table 1, where PVR is a precision voltage reference (LM4050-10 [9]). The output voltage of PVR is stable 10 V with typical error of ± 40 ppm. The noises from PVR are eliminated by C_1, C_2, and R_{T}. Here, $R_{\mathrm{T}} = R_{\mathrm{t}} + R_{\mathrm{t1}}$, and R_{t1} is a variable resistor. Keep R_{p} to 0, and adjust R_{s1}, R_{h1}, and R_{t1} to achieve JFET at the ideal operating point ($V_{\mathrm{ds}} = 1$ V, $I_{\mathrm{ds}} = 1$ mA) and the voltage at O1 equal to that at O2. The performances of Pre-Amp measured at 77K are shown in Table 1.

For Pre-Amp, adding AC voltage signal $\dot{V}$ on G, the output AC voltage signal difference between O1 and O2 is $\dot{V}_{\mathrm{pre}}$. The gain of Pre-Amp is $A_{\mathrm{vP}} = \dot{V}_{\mathrm{op}}/\dot{V}$. The upper limit cutoff frequency for Pre-Amp is larger than 5 MHz, since the transit frequency for JFET is $g_{\mathrm{m}}/(2\pi C_{\mathrm{gs}})$ is larger than 200 MHz and the intrinsic gain for JFET $g_{\mathrm{m}}/g_{\mathrm{d}} < 30$. For Pre-Amp, A_{vP} can be obtained by the nodal analysis method [1]. In $f >> \max\{g_{\mathrm{m}}/(2\pi C_{\mathrm{S}}), 1/(2\pi R_{\mathrm{S}} C_{\mathrm{S}})\}$ (i.e. $f >> 12$ Hz) and $f \leq 1$ MHz, A_{vP} is

$$A_{\mathrm{vP}} \approx -g_{\mathrm{m}} R_{\mathrm{d}}, \tag{2.1}$$

and $A_{\mathrm{vP}} \approx -14.4$ (with the parameters in Table 1), where $R_{\mathrm{d}} = R_{\mathrm{L}}/(1 + R_{\mathrm{L}} g_{\mathrm{d}})$. The input capacitance of Pre-Amp is

$$C_{\mathrm{A}} = C_{\mathrm{gs}} + (1 - A_{\mathrm{vP}}) C_{\mathrm{gd}}. \tag{2.2}$$

Table 1: Parameters of all components of TJ-TIA

JFET SST4393-T1			
Gate–source resistance R_{A}			>10 TΩ
Transconductance g_{m}			8 mS
Channel conductance g_{d}			0.3 mS
Gate–source capacitance C_{gs}			9 pF
Gate–drain capacitance C_{gd}			5 pF
Drain–source voltage V_{ds}			1 V
Drain–source current I_{ds}			1 mA
$\overline{e_{\mathrm{J}}^2}$ ((nV)^2/Hz)		10 kHz	7
		50 kHz	3
$\overline{i_{\mathrm{J}}^2}$ ((fA)^2/Hz)		unkown	
Pre-Amp			
$R_{\mathrm{s}} + R_{\mathrm{s1}}$	520 ± 5 Ω	C_{S}	11 μF
$R_{\mathrm{h}} + R_{\mathrm{h1}}$	1520 ± 5 Ω	R_1, R_2	3.9 kΩ
R_{p}	5±5 Ω		
C_1	22 μF	C_2	11 μF
PVR	LM4050-10	R_{b}	2 kΩ
$R_{\mathrm{t}} + R_{\mathrm{t1}}$	2280 ± 10 Ω	V_{Pp}	+15 V
Post-Amp with THS4021 as Rear-OPA			
a_{a0}	94 dB	f_{b}	16 kHz
C_{a}	1.5 pF	R_{a}	1 MΩ
R_{f}	3.9 MΩ	C_{i1}, C_{i2}	160 pF
R_{c1},R_{c2}	100 Ω	C_{r1}, C_{r2}	50 pF
V_{Rp}	+5 V	V_{Rn}	-5 V
Feedback network			
R_{F}	1.13 GΩ	C_{F}	~ 3 pF
R_{k}	340 kΩ	C_{k}	~ 0.2 pF
C_{c}	10 nF		
Signal source circuit			
R_{J}	3.9 MΩ	C_{I}	~ 0.1 pF

Note: ± indicates the variable resistance range. Without specification, the default value after ± is 0.

and $C_{\mathrm{A}} \approx 81$ pF (with the parameters in Table 1). The input resistance of Pre-Amp R_{A} is the gate-source resistance of JEFT. For SST4393-T1, $R_{\mathrm{A}} > 1$ TΩ, so R_{A} can be considered as infinity.

2.2 Post-Amplifier and Invertin-Amplifier

Fig.1(b) shows the Post-Amp circuit. An operational amplifier (OPA) is in the circuit, denoted as Rear-OPA. Rear-OPA used in this work is THS4021 [11]. R_{a} and C_{a} are the equivalent input resistance and capacitance of Rear-OPA, respectively. The positive input of Rear-OPA is connected with a filter composed of R_{c1} and C_{r1}, which is connected to the inverting output of Pre-Amp O1 with Cable O1Q1. The inverting input of Rear-OPA is connected with a filter composed of R_{c2} and C_{r2}, which is connected to the positive output of Pre-Amp O2 with Cable O2Q2. The ground capacitances of Cable O1Q1 and Cable O2Q2 are C_{i1} and C_{i2} respectively. The lengths of Cable O1Q1 and Cable O2Q2 are 1.6 m, and $C_{\mathrm{i1}} = C_{\mathrm{i2}} = C_{\mathrm{i}}$ is about 160 pF. The feedback resistor R_{f} is connected to the output of Rear-OPA O to O2.

In Post-Amp, $V_{\rm Rp}$ is set at +5 V and $V_{\rm Rn}$is set at -5 V, since the input voltage range of the oscilloscope (Rohde-Schwarz RTP) used in measurements is ±5 V. And, $V_{\rm Rp}$ ($V_{\rm Rn}$) can be set at +15 V (-15 V) for the real application.

Cascade Pre-Amp and Post-Amp to form Inv-Amp. For the AC signal, the voltage gain of Inv-Amp $a_{\rm A}(f)$ can be expressed as

$$a_{\rm A} = A_{\rm vP} A_{\rm vR}. \tag{2.3}$$

$a_{\rm A}$ can be obtained with the nodal analysis method, and then $A_{\rm vR}$ can be obtained [1, 10]. In $f >> \max\{g_{\rm m}/(2\pi C_{\rm S}), 1/(2\pi R_{\rm S} C_{\rm S})\}$(i.e. $f >> 12$ Hz) and $f \leq 1$ MHz, $A_{\rm vR}$ is

$$A_{\rm vR} \approx \frac{Z_{\rm f}}{R_{\rm HL}} \cdot \frac{1 + j2\pi f R_{\rm HL} C_{\rm ir}}{1 + j2\pi f R_{\rm d} C_{\rm ir}} \cdot \frac{1}{1 + \frac{Z_{\rm f}}{a_{\rm a} R_{\rm HL}} + j2\pi f \frac{Z_{\rm f} C_{\rm ir}}{a_{\rm a}}}, \tag{2.4}$$

where $Z_{\rm f} = 1/(1/R_{\rm f} + j2\pi f C_{\rm f})$, $R_{\rm HL} = R_{\rm H} R_{\rm L}/(R_{\rm H} + R_{\rm L})$, $C_{\rm ir} = C_{\rm i} + C_{\rm r}$, and $a_{\rm a}$ is the voltage gain of the Rear-OPA. For THS4021, in $0 < f \leq 1$ MHz, $a_{\rm a} \approx a_{\rm a0}/(1 + jf/f_{\rm b})$, where $a_{\rm a0} = 94$ dB, $f_{\rm b} = 16$ kHz.

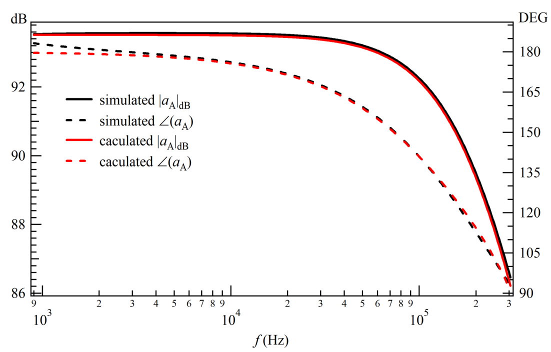

Figure 2: For the voltage gain of Inv-Amp $a_{\rm A}(f)$, the simulated $|a_{\rm A}(f)|_{\rm dB}$ vs. f is the black solid curve and the simulated $\angle(a_{\rm A}(f))$ vs. f is the black dashed curve. By Eq.(2.1), (2.3), and (2.4), the calculated $|a_{\rm A}(f)|_{\rm dB}$ vs. f is the red solid curve and the calculated $\angle(a_{\rm A}(f))$ vs. f is the red dashed curve.

With the parameters in Table 1, the performances of Inv-Amp are simulated with TINA-TI [12]. The simulated results of $a_{\rm A}(f)$ are shown as the black curves in Fig.2. The results of $a_{\rm A}(f)$ calculated by Eq.(2.1), (2.3), and (2.4) are shown as the red curves in Fig..2, which are basically consistent with the simulated ones in 3 kHz$< f \leq 300$ kHz.

$a_{\rm A}(f)$ is measured by a lock-in (Standford 865). In 100 Hz$< f < 240$ kHz, the measured results of $a_{\rm A}(f)$ are also basically consistent with those obtained by TINA-TI simulation, as shown in Fig.3. Because the voltage gain of Inv-Amp is higher than 50,000, the crosstalk signal can be easily introduced to its input G at 77 K through the cable between the inut G and the output of the lock-in. Therefore, the fluctuations of the measured $|a_{\rm A}(f)|_{\rm dB}$ are quite large. We should note that the cable between the inut G and the output of the lock-in is only used for the Inv-Amp voltage gain measurements and it should not be there for TIA.

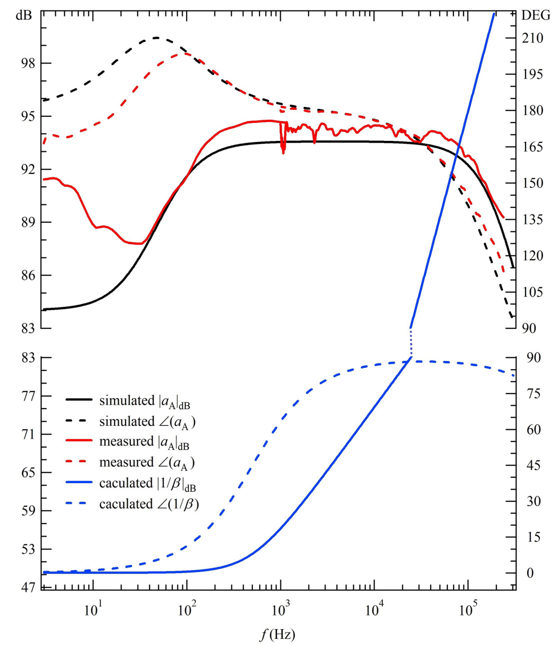

Figure 3: The simulated results and measured results for the voltage gain of Inv-Amp $a_{\mathrm{A}}(f)$, and the calculated results for the reciprocal of the feedback factor of TJ-TIA $1/\beta(f)$. For $R_{\mathrm{J}} = 3.9$ MΩ, $|T_{\mathrm{L}}|_{\mathrm{dB}} = |a_{\mathrm{A}}|_{\mathrm{dB}} - |1/\beta(f)|_{\mathrm{dB}} \leq -10$ dB in $f \geq 243$ kHz, and $\angle(T_{\mathrm{L}}) = \angle(-a_{\mathrm{A}}) - \angle(1/\beta) = \angle(a_{\mathrm{A}}) - 180^{\circ} - \angle(1/\beta) > -139^{\circ}$ in $f < 243$ kHz. The gain margin for stability of TJ-TIA is larger than 10 dB and the phase margin is larger than 41°.

2.3 Frequency compensation of feedback loop

Fig.1(c) shows the feedback network in TIA. It compensates the frequency of the feedback resistance R_{F} according to the method described in Ref.[1]. The feedback impedance obtained by compensation is

$$Z_{\mathrm{F}}(f) \approx \frac{R_{\mathrm{k}} + R_{\mathrm{F}}}{1 + j2\pi f R_{\mathrm{k}} C_{\mathrm{k}}} \approx \frac{R_{\mathrm{F}}}{1 + j2\pi f R_{\mathrm{k}} C_{\mathrm{k}}},$$

$f_{\mathrm{F}} = 1/(2\pi f R_{\mathrm{k}} C_{\mathrm{k}})$ is the upper cut-off frequency of the feedback network. Here $R_{\mathrm{F}} = 1.13$ GΩ at 77 K. A small 2.7 pF capacitor is parallel to R_{F} with about 0.3 pF parasitic capacitance, therefore C_{F} as the total capacitance parallel to R_{F} is about 3 pF. $C_{\mathrm{c}} = 10$ nF, and $R_{\mathrm{k}} C_{\mathrm{c}} \sim R_{\mathrm{F}} C_{\mathrm{F}}$ as adjusting resistance $R_{\mathrm{k}} = 340$ kΩ. The measured results for $Z_{\mathrm{F}}(f)$ are shown in Fig.4, and f_{F} is up to 2.25 MHz.

2.4 Stibility of TJ-TIA

Fig.1(d) shows the signal source circuit. The differential resistance of TJ in CryoSTM is denoted as R_{J}. In this work, a resistor of 3.9 MΩ is used as R_{J} instead of TJ between A and B. The capacitance of TJ is denoted as C_{J}, which is in parallel with R_{J}. $C_{\mathrm{J}} \leq 100$ fF for the resistor of 3.9 MΩ, and it is estimated as only several fF for TJ in CryoSTM [2]. $C = C_{\mathrm{A}} + C_{\mathrm{I}} + C_{\mathrm{J}}$ in this work. C_{J} is at least two orders of magnitude less than $C_{\mathrm{A}} + C_{\mathrm{I}}$,

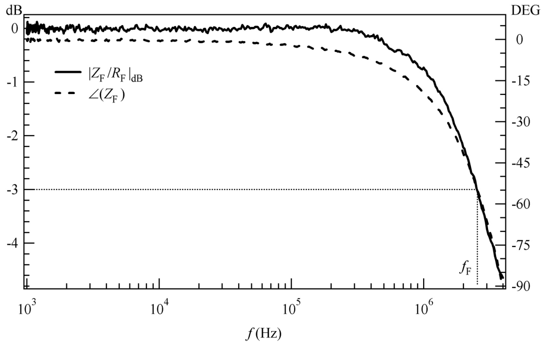

Figure 4: The measured $|Z_{\mathrm{F}}(f)/R_{\mathrm{F}}|_{\mathrm{dB}}$ (Solid curve) and the measured $\angle(Z_{\mathrm{F}}(f))$ (Dashed curve). f_{F} is up to 2.25 MHz.

so it can be ignored in C. The DC bias-modulated signal voltage source is denoted as BMS. TIA connects the signal source circuit to form TJ-TIA.

The loop gain T_{L} of TJ-TIA is

$$T_{\mathrm{L}} = -a_{\mathrm{A}}(f)\beta(f) = -a_{\mathrm{A}}/(1/\beta), \tag{2.5}$$

in which $\beta(f)$ is the feedback factor. And, its reciprocal is

$$1/\beta(f) = 1 + Z_{\mathrm{F}}(f)\left[1/Z_{\mathrm{J}}(f) + j2\pi fC\right],$$

where $Z_{\mathrm{F}}(f) = R_{\mathrm{F}}/(1 + j2\pi fR_{\mathrm{k}}C_{\mathrm{k}})$ and $Z_{\mathrm{J}}(f) = R_{\mathrm{J}}/(1 + j2\pi fR_{\mathrm{J}}C_{\mathrm{J}})$. Since $C_{\mathrm{I}} \leq 0.5$ pF and $C_{\mathrm{A}} \approx 81$ pF,

$$1/\beta(f) = 1 + Z_{\mathrm{F}}(f)(1/Z_{\mathrm{J}} + j2\pi fC_{\mathrm{A}}). \tag{2.6}$$

With the parameters in Table 1, the performance of TJ-TIA is simulated and calcultated with TIN-TI. For Inv-Amp, Fig.5 shows the curves of $|a_{\mathrm{A}}(f)|_{\mathrm{dB}}$ and $\angle(aA(f))$ simullated by TINA-TI. In Fig.5, the curves of $|1/\beta(f)|_{\mathrm{dB}}$ and $\angle(1/\beta(f))$ are obtained with Eq.(2.6).It is obtained that $|T_{\mathrm{L}}(f)|_{\mathrm{dB}} = |a_{\mathrm{A}}(f)|_{\mathrm{dB}} - |1/\beta(f)|_{\mathrm{dB}} \leq -10$ dB as $f \geq 180$ kHz, and $\angle(T_{\mathrm{L}}(f)) = \angle(-aA(f)) - \angle(1/\beta(f)) = \angle(aA(f)) - 180^\circ - \angle(1/\beta(f)) > -139^\circ$. Therefore, TJ-TIA circuit is stable with a gain margin of stability greater than 10 dB and a phase margin greater than 41°. For $R_{\mathrm{J}} \geq 1$ MΩ, it can be easily to verify that the curves of $|a_{\mathrm{A}}(f)|_{\mathrm{dB}}$ and $|1/\beta(f)|_{\mathrm{dB}}$ are basically the same as those in Fig.5 in $f > 10$ kHz, and that $\angle(1/\beta(f)) < 90^\circ$ and $\angle(aA(f)) > 150^\circ$ in $f < 10$ kHz [1]. Therefore, the TJ-TIA circuit is stable as $R_{\mathrm{J}} \geq 1$ MΩ, and the stability margin is the same as that as $R_{\mathrm{J}} \geq 3.9$ MΩ.

In experiments, as the input of TIA is short, the output voltage of TIA can be set and kept at 0 after well-calibration, and no oscillation signal is found. In Section 2.5, there is no "gain peaking" on the measuerd curve for the modulus of transimpedance gain of TJ-TIA with $R_{\mathrm{J}} = 3.9$ MΩ. These phenomena also confirm the stability of TJ-TIA.

2.5 Transimpedance gain of TIA

With the frequency compensation as mentioned in Section 2.3, it can be considered that Z_{F} is equal to R_{F} in $0 < f \leq 300$ kHz. Considering the TJ capacitance C_{J}, the TJ

impedance is $Z_\mathrm{J} = R_\mathrm{J}/(1 + j2\pi f R_\mathrm{J} C_\mathrm{J})$. In $0 < f \leq 300$ kHz, for $R_\mathrm{J} \geq 1$ MΩ, the transimpedance gain of TIA A_i is [1]

$$A_\mathrm{i} = -\frac{R_\mathrm{F}}{1 - \frac{1}{a_\mathrm{A}} - \frac{R_\mathrm{F}}{a_\mathrm{A} R_\mathrm{A}} - j2\pi f \frac{R_\mathrm{F} C_\mathrm{A}}{a_\mathrm{A}}},$$

Considering $R_\mathrm{A} >> R_\mathrm{F}$ and $|a_\mathrm{A}| >> 1$, A_i is

$$A_\mathrm{i} = -\frac{R_\mathrm{F}}{1 - j2\pi f \frac{R_\mathrm{F} C_\mathrm{A}}{a_\mathrm{A}}}, \tag{2.7}$$

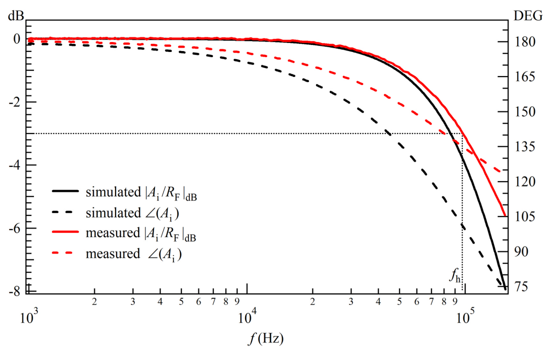

Figure 5: For the transimpedance gain of TIA A_i, the simulated $|A_\mathrm{i}(f)/R_\mathrm{F}|_\mathrm{dB}$ (Black solid curve) and the simulated $\angle(A_\mathrm{i}(f))$ (Black dashed curve), and the measured $|A_\mathrm{i}(f)/R_\mathrm{F}|_\mathrm{dB}$ (Red solid curve) and the measured $\angle(A_\mathrm{i}(f))$ (Red dashed curve).

It is easily to verify that the caculated results of A_i by Eq.(2.7) are consistent with the simulated results with TINA-TI [1]. For the TJ-TIA, A_i with $R_\mathrm{J} = 3.9$ MΩ (with $C_\mathrm{J} \leq 100$ fF) is measured by a lock-in (Standford 865). Fig.5 shows the measured results and simulated results. The measured bandwidth of TIA f_h is about 97 kHz, while the simulated one is 86 kHz.

3 Noise performences of TIA

For the circuit of TJ-TIA shown in Fig.1, we use the differential equivalent circuit with all noise sources to calculate its equivalent input noise. The details for the noise calculations are shown in Supplemental file [13]. In this work, the noise voltage PSD is measured by a vector analyzer (Agilent 89441A) or a oscilloscope (Rohde-Schwarz RTP).

3.1 Equivalent input noises of Inv-Amp

The equivalent input noise voltage and equivalent input noise current of JFET are denoted as e_J and i_J respectively. They may not independent. The equivalent input noise voltage and equivalent input noise current of the Rear-OPA are denoted as e_a and i_a respectively. They may not independent, but they are commonly considered as independent.

The resistors R_s, R_1, R_2, R_h, and R_f are in the cryogenic zone of 4.2 K. R_h is in the cryogenic zone of 77 K, the noise voltage of the resistor R_H is e_RH. , And, their noises in

$f > 1$ kHz are thermal noise, which can be neglected [1]. The noise voltage of the resistor R_{c1} is e_1, and that of R_{c2} is e_2. And, their noises in $f > 1$ kHz are thermal noise. These noise sources are independent. The equivalent input noise voltage and equivalent input noise current of Inv-Amp are denoted as e_{A} and i_{A} respectively. By the nodal analysis method and Wiener-Sinchin theorem, ignoring the minor terms, it is obtained that [13]

$$\overline{e_{\mathrm{A}}^2} = \overline{e_{\mathrm{J}}^2} + \left(\overline{e_{\mathrm{a}}^2} + \overline{e_1^2} + \overline{e_2^2}\right)/A_{\mathrm{vP}}^2, \tag{3.1}$$

$$\begin{aligned}\overline{i_{\mathrm{A}}^2} = \overline{i_{\mathrm{J}}^2} &+ (2\pi f)^2 \frac{C_{\mathrm{A}}^2}{A_{\mathrm{vP}}^2}\left(\frac{R_{\mathrm{HL}}^2}{R_{\mathrm{H}}^2}\overline{e_{\mathrm{RH}}^2} + \overline{e_{\mathrm{a}}^2} + \overline{e_1^2} + \overline{e_2^2}\right)\\ &+(2\pi f)^2\left(C_{\mathrm{gs}} + C_{\mathrm{gd}} + \frac{R_{\mathrm{HL}}}{R_{\mathrm{d}}}C_{\mathrm{A}}\right)^2\frac{\overline{i_{\mathrm{a}}^2}}{g_{\mathrm{m}}^2},\end{aligned} \tag{3.2}$$

$$\begin{aligned}\overline{e_{\mathrm{A}} i_{\mathrm{A}}^*} =&(\overline{i_{\mathrm{A}} e_{\mathrm{A}}^*})^* = -j2\pi f\frac{C_{\mathrm{A}}}{A_{\mathrm{vP}}^2}\left(\frac{R_{\mathrm{HL}}^2}{R_{\mathrm{H}}^2}\overline{e_{\mathrm{RH}}^2} + \overline{e_{\mathrm{a}}^2} + \overline{e_1^2} + \overline{e_2^2}\right)\\ &- j2\pi f\left(C_{\mathrm{gs}} + C_{\mathrm{gd}} + \frac{R_{\mathrm{HL}}}{R_{\mathrm{d}}}C_{\mathrm{A}}\right)\left(1 + \frac{R_{\mathrm{HL}}}{R_{\mathrm{d}}}\right)\frac{\overline{i_{\mathrm{a}}^2}}{g_{\mathrm{m}}^2},\end{aligned} \tag{3.3}$$

where $\overline{e_{\mathrm{A}}^2}$ is the equivalent input noise voltage PSD of Inv-Amp, $\overline{i_{\mathrm{A}}^2}$ is its equivalent input noise current PSD, $\overline{e_{\mathrm{A}} i_{\mathrm{A}}^*}$ is its equivalent input noise voltage-current PSD, and $\overline{i_{\mathrm{A}} e_{\mathrm{A}}^*}$ is its equivalent input noise current-voltage PSD.

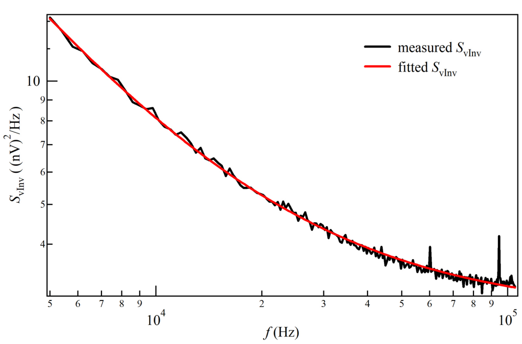

Figure 6: The measured equivalent input noise voltage PSD of Inv-Amp $S_{\mathrm{vInv}} = \overline{e_{\mathrm{A}}^2}$. It is about 8 (nV)^2/Hz at $f = 10$ kHz and 3.7 (nV)^2/Hz at $f = 50$ kHz.

The output noise voltage PSD of Inv-Amp S_{oInv} is measured. And, its equivalent input noise voltage PSD S_{vInv} is obtained as $S_{\mathrm{vInv}} = S_{\mathrm{oInv}}/|a_{\mathrm{A}}|^2$, and $S_{\mathrm{vInv}} = \overline{e_{\mathrm{A}}^2}$. Fig.6 shows the curve for S_{vInv} vs. f. In Fig.6, $S_{\mathrm{vInv}} = \overline{e_{\mathrm{A}}^2}$ is about 8 (nV)^2/Hz at $f = 10$ kHz and 3.7 (nV)^2/Hz at $f = 50$ kHz, which are consistent with the values obained from Eq.(3.1) with the parameters in Table 1.

For TIA, its equivalent input noise voltage and equivalent input noise current are denoted as e_{T} and i_{T} respectively. The equivalent input noise voltage PSD of TIA $\overline{e_{\mathrm{T}}^2}$, its equivalent input noise current PSD $\overline{i_{\mathrm{T}}^2}$, its equivalent input noise voltage-current PSD $\overline{e_{\mathrm{A}} i_{\mathrm{A}}^*}$, and its equivalent input noise current-voltage PSD $\overline{i_{\mathrm{A}} e_{\mathrm{A}}^*}$ are [1, 13]

$$\overline{e_{\mathrm{T}}^2} = \overline{e_{\mathrm{A}}^2}, \tag{3.4}$$

$$\overline{i_{\mathrm{T}}^2} = \overline{i_{\mathrm{A}}^2} + 4k_{\mathrm{B}}T/R_{\mathrm{F}}, \tag{3.5}$$

$$\overline{e_{\mathrm{T}} i_{\mathrm{T}}^*} = (\overline{i_{\mathrm{T}} e_{\mathrm{T}}^*})^* = \overline{e_{\mathrm{A}} i_{\mathrm{A}}^*}. \tag{3.6}$$

Therefore, the measured $\overline{e_{\mathrm{T}}^2}$ is about $8(\mathrm{nV})^2/\mathrm{Hz}$ at $f = 10$ kHz and 3.7 $(\mathrm{nV})^2/\mathrm{Hz}$ at $f = 50$ kHz.

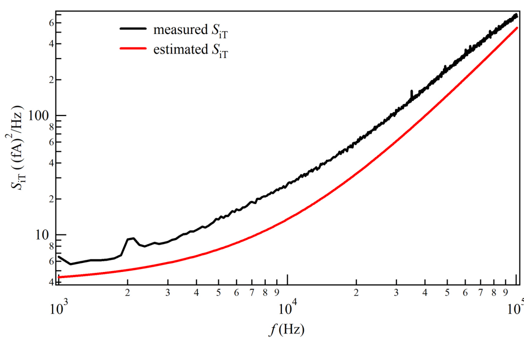

Figure 7: The measured equivalent input noise current PSD of TIA $S_{\mathrm{iT}} = \overline{i_{\mathrm{T}}^2}$. It is about 26 $(\mathrm{fA})^2/\mathrm{Hz}$ at $f = 10$ kHz and 240 $(\mathrm{fA})^2/\mathrm{Hz}$ at $f = 50$ kHz.

In Fig.7, the black curve is the measured equivalent input noise current PSD of TIA $S_{\mathrm{iT}} = \overline{i_{\mathrm{T}}^2}$ as the input TIA is opened. The measured values are 26 $(\mathrm{fA})^2/\mathrm{Hz}$ at $f = 10$ kHz and 240 $(\mathrm{fA})^2/\mathrm{Hz}$ at $f = 50$ kHz. It is difficult to obtain the equivalent input noise current PSD of JFET $\overline{i_{\mathrm{J}}^2}$ by measurements [7]. Let's assume that $\overline{i_{\mathrm{J}}^2}$ is the ideal minimum one. In this case, it is entirely generated by the channel noise current PSD of JFET i_{c}. It can be obtained that $\overline{e_{\mathrm{J}}^2} \approx \overline{i_{\mathrm{c}}^2}/g_{\mathrm{m}}^2$ [**?**]. Therefore [**?**],

$$\overline{i_{\mathrm{J}}^2} \approx (2\pi f)^2 \left(C_{\mathrm{gs}} + C_{\mathrm{gd}}\right)^2 \overline{i_{\mathrm{c}}^2}/g_{\mathrm{m}}^2 \approx (2\pi f)^2 \left(C_{\mathrm{gs}} + C_{\mathrm{gd}}\right)^2 \overline{e_{\mathrm{J}}^2}. \tag{3.7}$$

Based on this assumption, $S_{\mathrm{iT}} = \overline{i_{\mathrm{T}}^2}$ is estimated by Eq.(3.2), (3.5) and (3.7), with the parameters in Table 1, and the results are shown as the red curve in Fig7. The estimated values are $13.7(\mathrm{fA})^2/\mathrm{Hz}$ at $f = 10$ kHz and $148(\mathrm{fA})^2/\mathrm{Hz}$ at $f = 50$ kHz. The estimated valus of S_{iT} are slightly smaller than the measured ones, since we assume $\overline{i_{\mathrm{J}}^2}$ as the ideal minimum one.

In summary, for the TIA in this work, its equivalent input noise voltge PSD is about $8(\mathrm{nV})^2/\mathrm{Hz}$ at $f = 10$ kHz and 3.7 $(\mathrm{nV})^2/\mathrm{Hz}$ at $f = 50$ kHz, and its equivalent input noise current PSD is 26 $(\mathrm{fA})^2/\mathrm{Hz}$ at $f = 10$ kHz and 240 $(\mathrm{fA})^2/\mathrm{Hz}$ at $f = 50$ kHz. Considering the bandwidth of TIA about 97 kHz and its gain of 1.13 GΩ, the TIA in this work has the lowest noise and largest bandwidth among the present low-noise large-bandwidth high-gain TIAs [3, 14, 15].

4 Transimpedance gain of TIA obtained with noise measurements

In the TJ-TIA, the resistor of 3.9 MΩ is used as R_{J} instead of TJ between A and B, and B is grounded. Its thermal noise voltage PSD $S_{\mathrm{RJ}} = 4k_{\mathrm{B}}T/R_{\mathrm{J}} = 1090$ $(\mathrm{fA})^2/\mathrm{Hz}$. The

output noise voltage of TJ-TIA $S_{\mathrm{oTJ}}(f)$ is measured in 500 Hz< $f \leq 100$ kHz. Obviously,

$$|A_{\mathrm{i}}|^2 = \frac{S_{\mathrm{oTJ}}(f) - S_{\mathrm{oT}}(f)}{4k_{\mathrm{B}}T/R_{\mathrm{J}}}. \tag{4.1}$$

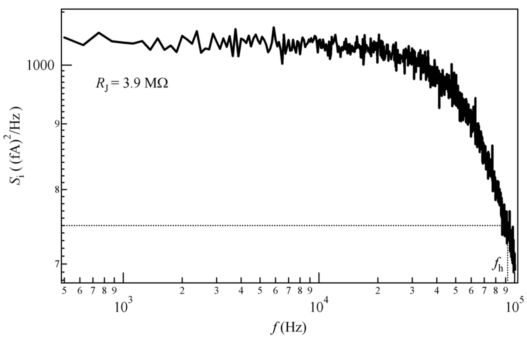

Figure 8: In the TJ-TIA, for a resistor R_{J} of 3.9 MΩ, the measured resullts for $S_{\mathrm{i}} = |A_{\mathrm{i}}/R_{\mathrm{F}}|^2 S_{\mathrm{RJ}}$ in 500 Hz< $f \leq 100$ kHz. The measured bandwidth of TIA f_{h} is about 92 kHz.

Fig.8 shows the measured resullts for $S_{\mathrm{i}} = |A_{\mathrm{i}}/R_{\mathrm{F}}|^2 S_{\mathrm{RJ}}$ in 500 Hz< $f \leq 100$ kHz. In Fig.8, the measured thermal noise voltage PSD S_{RJ} at 1 kHz is about 1050 (fA)^2/Hz. With this meathod, the measured bandwidth of TIA f_{h} is about 92 kHz, which is approximate to the value of 97 kHz measured by the lock-in in Section 2.5.

5 Conclusion

In Ref.[1, 2], the designs of low-noise large-bandwidth high-gain transresistance amplifier (TIA) for Cryogenic STM are proposed and their performances are verified with simulations and theoretical calculations. In this work, for the design of TIA in Ref.[1], we replace the expensive CHRS-HEMT with a junction field-effect transistor (JFET) SST4393-T1 that can operate at 77K. Based on the same design ideas, methods, and theoretical calculations, we design, fabricate, and measure TIA with the same circuit topology as that in Ref.[1]. The measured performances of TIA are in agreement with the simulated and calculated results, therefore the feasibility of the TIA design in Ref.[1] is verified. The transimpedance gain of TIA is 1.13 GΩ and its bandwidth is 97 kHz. its equivalent input noise voltage PSD is about 8 (nV)^2/Hz at 10k Hz and 3.7 (nV)^2/Hz at 50kHz, and its equivalent input noise current PSD is about 26 (fA)^2/Hz at 10 kHz and 240 (fA)^2/Hz at 50 kHz. TIA in this work can be used in CryoSTM at 77 K(liquid nitrogen temperature).

Acknowledgment

This work is supported by Open Research Fund Program of the State Key Laboratory of Low-Dimensional Quantum Physics (Grant No. KF202212).

Declaration of competing interest

The author declares that they have no known competing financial interests or personal relationships that could have appeared to influence the work reported in this paper.

References

[1] Y.X. Liang, Ultra-low-noise transimpedance amplifier with a single HEMT in preamplifier for measuring shot noise in cryogenic STM, submitted to Ultramicroscopy, https://chinaxiv.org/abs/202212.00178?locale=en.

[2] Y.X. Liang, Low-noise large-bandwidth tansimpedance amplifier for measuring scanning tunneling shot noise spectra in cryogenic STM and its applications, Ultramicroscopy 234 (2022) 13466, https://doi.org/10.1016/j.ultramic.2022.113466.

[3] Data sheet of FEMTO DE-DLPCA-200 variable gain low noise current amplifier, https://www.femto.de/images/pdfdokumente/de-dlpca-200.pdf.

[4] Y.X. Liang, Low-noise high-gain large-bandwidth transimpedance amplifier with cascode-type preamplifier for cryogenic STM, J. Low Temp. Phys 210 (2023) 357, https://doi.org/10.1007/s10909-022-02855-0.

[5] Y.X. Liang, Ultra-low-noise transimpedance amplifier in cryogenic STM for studying novel quantum states by measuring shot noise, Low Temp. Phys 49 (2023) 676, https://doi.org/10.1063/10.0017824.

[6] Y.X. Liang, Q. Dong, M.C. Cheng, U. Gennser, A. Cavanna, and Y. Jin, Insight into low frequency noise induced by gate leakage current in AlGaAsGaAs high electron mobility transistors at 4.2 K, Appl. Phys. Lett. 99 (2011) 113505, https://doi.org/10.1063/1.3637054.

[7] Y. Jin, Q. Dong, A. Cavanna, U. Gennser, L. Couraud, and C. Ulysse, Ultra-low noise HEMTs for deep cryogenic low-frequency and highimpedance readout electronics, 12th IEEE International Conference on Solid-State and Integrated Circuit Technology (ICSICT) (2014).

[8] Data sheet of SST4393, https://www.alldatasheet.com/datasheet-pdf/pdf/600354/VISHAY/SST4393.html.

[9] Data sheet of LM4050-10, https://www.ti.com.cn/document-viewer/cn/lm4050-n/datasheet.

[10] Supplemental file 1.

[11] Data sheet of THS4021 OPA, https://www.ti.com/lit/ds/symlink/THS4021.pdf.

[12] TINA-TI is SPICE-based analog simulation program produced by Texas Instruments Inc., https://www.ti.com/tool/TINA-TI.

[13] Supplemental file 2.

[14] M. Stubian, J. Bobek, M. Setvin, U. Diebold, and M. Schmid, Fast low-noise ransimpedance amplifier for scanning tunneling microscopy and beyond, Rev. Sci. Instrum. 91, (2020). 074701.

[15] For AD8615, the typical value of its equivalent input noise voltage PSD is 40 $(\mathrm{nV})^2/\mathrm{Hz}$ in $f > 10$ kHz, and the typical value of its equivalent input noise current PSD is 2500 $(\mathrm{fA})^2/\mathrm{Hz}$ at $f = 1$ kHz. And, its equivalent input noise current PSD should be increased with the increase of frequency. For TIA with AD8615 as Pre-Amplifier in Marcro-OPA, its equivalent input noise voltage (current) PSD cannot be lower than that of AD8615. Data sheet of AD8615, https://www.analog.com/media/en/technical-documentation/data-sheets/AD8615_8616_8618.pdf.

Supplemental file 1: Voltage gain of Inv-Amp

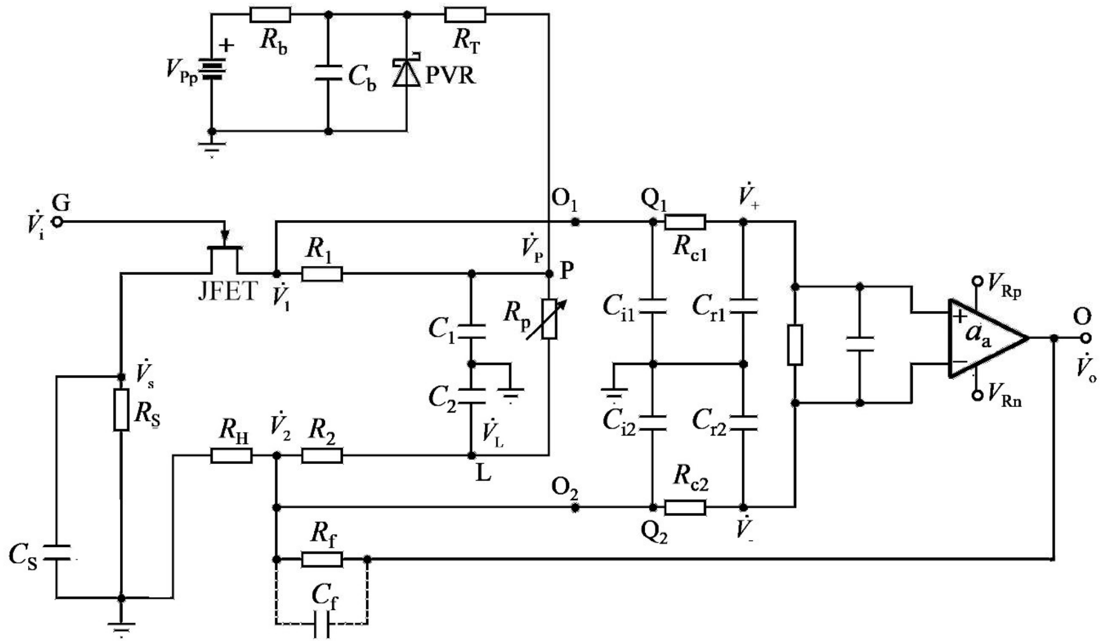

Figure s1.1 The Inv-Amp circuit with all components for Eqs.(s1.1-s1.8), and their values are shown in Table 1 in Article.

With the nodal analysis method, the Inv-Amp voltage gain $a_A(f)$ is calculated by the following equations. All components for Eqs.(s1.1-s1.9) are shown in Fig.s1.1, and their values are shown in Table 1 in Article.

$$\left(\dot{V}_o-\dot{V}_2\right)\Big/R_f=\left(\dot{V}_2-\dot{V}_L\right)\Big/R_2+\left(\dot{V}_2-\dot{V}_-\right)\Big/R_{c2}+\dot{V}_2/R_H+j\omega C_{i2}\dot{V}_2\,, \tag{s1.1}$$

$$j\omega C_{gd}\left(\dot{V}_i-\dot{V}_1\right)=g_m\left(\dot{V}_i-\dot{V}_s\right)+g_d\left(\dot{V}_1-\dot{V}_s\right)+\left(\dot{V}_1-\dot{V}_P\right)\Big/R_1+\left(\dot{V}_1-\dot{V}_+\right)\Big/R_{c1}+j\omega C_i\dot{V}_2\,, \tag{s1.2}$$

$$\left(\dot{V}_1-\dot{V}_P\right)\Big/R_1+\left(\dot{V}_L-\dot{V}_P\right)\Big/R_p=\dot{V}_P/R_T+j\omega C_1\dot{V}_{tp}\,, \tag{s2.3}$$

$$\left(\dot{V}_2-\dot{V}_L\right)\Big/R_2=\left(\dot{V}_L-\dot{V}_P\right)\Big/R_p+j\omega C_2\dot{V}_L\,, \tag{s1.4}$$

$$g_m\left(\dot{V}_i-\dot{V}_s\right)+g_d\left(\dot{V}_1-\dot{V}_s\right)=\dot{V}_s/R_S+j\omega C_s\dot{V}_s+j\omega C_{gs}\left(\dot{V}_s-\dot{V}_i\right), \tag{s1.5}$$

$$\dot{V}_o=a_a\left(\dot{V}_+-\dot{V}_-\right), \tag{s1.6}$$

$$\left(\dot{V}_2-\dot{V}_-\right)\Big/R_{c2}=+j\omega C_{r2}\dot{V}_-\,, \tag{s1.7}$$

$$\left(\dot{V}_1-\dot{V}_+\right)\Big/R_{\mathrm{c1}}=+j\omega C_{\mathrm{r1}}\dot{V}_+\,, \tag{s1.8}$$

$$a_{\mathrm{A}}=\dot{V}_{\mathrm{o}}\Big/\dot{V}_{\mathrm{i}}\,, \tag{s1.9}$$

Supplemental file2: Noise of the proposed CryoSTM-TIA

S2-1 Noises of STM-TIA

For Inv-Amp, the equivalent input noise voltage of the Inv-Amp is denoted as e_{A} and its equivalent input noise current is i_{A}, and their harmonic components of frequency f are E_{A} and I_{A} respectively. $\begin{pmatrix} E_{\mathrm{A}} \\ I_{\mathrm{A}} \end{pmatrix}$ can be obtained by the nodal analysis method. By Wiener-Khintchine theorem, $\begin{pmatrix} \overline{e_{\mathrm{A}}^2} & \overline{e_{\mathrm{A}} i_{\mathrm{A}}^*} \\ \overline{i_{\mathrm{A}} e_{\mathrm{A}}^*} & \overline{i_{\mathrm{A}}^2} \end{pmatrix}$ can be obtained from $\begin{pmatrix} E_{\mathrm{A}} E_{\mathrm{A}}^* & E_{\mathrm{A}} I_{\mathrm{A}}^* \\ I_{\mathrm{A}} E_{\mathrm{A}}^* & I_{\mathrm{A}} I_{\mathrm{A}}^* \end{pmatrix}$ [S2R1, S2R2]. The two matrix elements on the main diagonal are the equivalent input noise voltage PSD of the Inv-Amp $\overline{e_{\mathrm{A}}^2}$ and its equivalent input noise current PSD $\overline{i_{\mathrm{A}}^2}$. The two matrix elements on the sub-diagonal are its equivalent input noise voltage-current PSD $\overline{e_{\mathrm{A}} i_{\mathrm{A}}^*}$ and equivalent input noise current-voltage PSD $\overline{i_{\mathrm{A}} e_{\mathrm{A}}^*}$.

The Inv-Amp is connected to the feedback resistor R_{F} to form a TIA. The equivalent input noise voltage of the TIA is denoted as e_{T} and its equivalent input noise current is i_{T}, and their harmonic components of f are E_{T} and I_{T} respectively. The temperature of the feedback resistance R_{F} is T, and its noise voltage is e_{F} and its harmonic component of f is E_{F}.

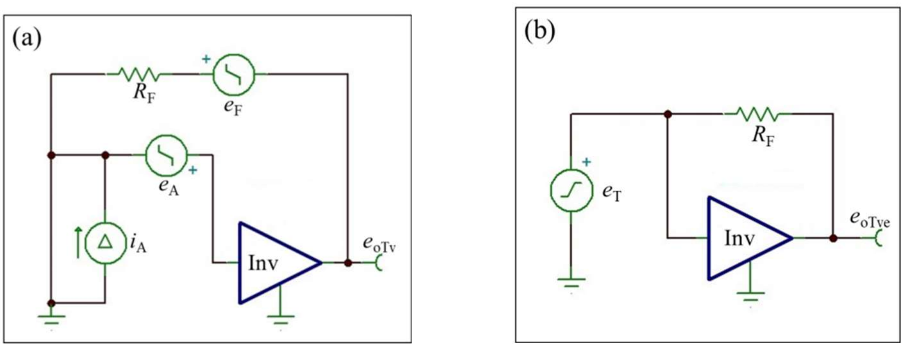

Figure s2.1 (a) TIA circuit with the input short-circuit containing the equivalent input noise voltage of Inv-Amp Inv e_{A} and its equivalent input noise current i_{A}, and the output noise voltage of e_{oTv} ; (b) Noiseless TIA circuit with the equivalent input noise voltage of the TIA e_{T} as the input signal, and the output noise voltage of e_{oTve} ; the equivalency of the above two circuits means $e_{\mathrm{oTv}} = e_{\mathrm{oTve}}$.

For the TIA, the circuit containing all noise sources with the input short-circuit is shown as Fig.s2.1(a), and the output noise is e_{oTv}. The noiseless circuit with the equivalent input noise voltage of the TIA e_{T} as the input signal is shown as Fig.s2.1(b), and the output noise is e_{oTve}. For calculating the equivalent input noise voltage of the TIA, the equations are established on the equivalency of the above two circuits, i.e. $e_{\mathrm{oTv}} = e_{\mathrm{oTve}}$. Therefore, by nodal analysis method,

$$E_{\mathrm{T}} = E_{\mathrm{A}} \,.$$

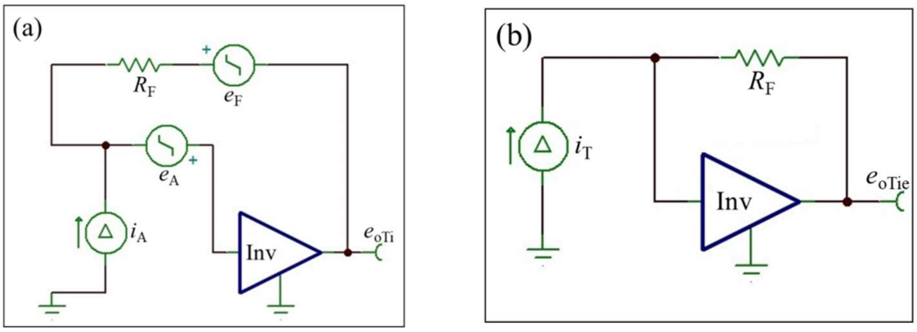

Figure s2.2 (a) TIA circuit with the input open-circuit containing the equivalent input noise current of Inv-Amp Inv e_{A} and its equivalent input noise current i_{A}, and the output noise current of e_{oTi}; (b) Noiseless TIA circuit with the equivalent input noise current of the TIA i_{T} as the input signal, and the output noise voltage of e_{oTie}; the equivalency of the above two circuits means $e_{\mathrm{oTi}} = e_{\mathrm{oTie}}$.

For the TIA, the circuit containing all noise sources with the input open-circuit is shown as Fig.s2.2(a), and the output noise is is e_{oTi}. The noiseless circuit with the equivalent input noise current of the TIA i_{T} as the input signal is shown as Fig.s2.2(b), and the output noise is e_{oTie}. For calculating the equivalent input noise current of the TIA, the equations are established on the equivalency of the above two circuits, i.e. $e_{\mathrm{oTi}} = e_{\mathrm{oTie}}$. Therefore, by the nodal analysis method,

$$I_{\mathrm{T}} = I_{\mathrm{A}} + (E_{\mathrm{A}} + E_{\mathrm{F}})/R_{\mathrm{F}} \,.$$

Hence,

$$\begin{pmatrix} E_{\mathrm{T}} \\ I_{\mathrm{T}} \end{pmatrix} = \begin{pmatrix} 0 \\ 1/R_{\mathrm{F}} \end{pmatrix} \left(E_{\mathrm{F}} + E_{\mathrm{A}} \right) + \begin{pmatrix} E_{\mathrm{A}} \\ I_{\mathrm{A}} \end{pmatrix} \,.$$

From $\begin{pmatrix} E_{\mathrm{T}}E_{\mathrm{T}}^{*} & E_{\mathrm{T}}I_{\mathrm{T}}^{*} \\ I_{\mathrm{T}}E_{\mathrm{T}}^{*} & I_{\mathrm{T}}I_{\mathrm{T}}^{*} \end{pmatrix}$, by Wiener-Khintchine theorem, $\begin{pmatrix} \overline{e_{\mathrm{T}}^{2}} & \overline{e_{\mathrm{T}}i_{\mathrm{T}}^{*}} \\ \overline{i_{\mathrm{T}}e_{\mathrm{T}}^{*}} & \overline{i_{\mathrm{T}}^{2}} \end{pmatrix}$ can be obtained.

The two matrix elements on the main diagonal are the equivalent input noise voltage

PSD of the TIA $\overline{e_{\mathrm{T}}^2}$ and its equivalent input noise current PSD $\overline{i_{\mathrm{T}}^2}$. The two matrix elements on the sub-diagonal are its equivalent input noise voltage-current PSD $\overline{e_{\mathrm{T}} i_{\mathrm{T}}^*}$ and equivalent input noise current-voltage PSD $\overline{i_{\mathrm{T}} e_{\mathrm{T}}^*}$.

$$\overline{e_{\mathrm{T}}^2} = \overline{e_{\mathrm{A}}^2} \quad , \tag{s2.1}$$

$$\overline{i_{\mathrm{T}}^2} = \overline{i_{\mathrm{A}}^2} + 4k_{\mathrm{B}}T/R_{\mathrm{F}} + \overline{e_{\mathrm{A}}^2}\big/R_{\mathrm{F}}^2 \quad , \tag{s2.2}$$

$$\overline{e_{\mathrm{T}} i_{\mathrm{T}}^*} = \left(\overline{i_{\mathrm{T}} e_{\mathrm{T}}^*}\right)^* \doteq \overline{e_{\mathrm{A}} i_{\mathrm{A}}^*} + \overline{e_{\mathrm{A}}^2}\big/R_{\mathrm{F}} \quad . \tag{s2.3}$$

Here, the noise voltage PSD of R_{F} is $\overline{e_{\mathrm{F}}^2} = 4k_{\mathrm{B}}TR_{\mathrm{F}}$.

The TIA is connected with the signal source circuit to form a STM-TIA. The equivalent input noise current PSD of a STM-TIA $\overline{i_{\mathrm{in}}^2}$ can be obtained [S2R1-S2R3] by

$$\overline{i_{\mathrm{in}}^2} = \overline{i_{\mathrm{T}}^2} + \left(1/R_{\mathrm{J}}^2 + (2\pi f)^2 C_{\mathrm{IJ}}^2\right)\overline{e_{\mathrm{T}}^2} + \left(1/R_{\mathrm{J}} + j2\pi f C_{\mathrm{IJ}}\right)\overline{e_{\mathrm{T}} i_{\mathrm{T}}^*} + \left(1/R_{\mathrm{J}} - j2\pi f C_{\mathrm{IJ}}\right)\overline{i_{\mathrm{T}} e_{\mathrm{T}}^*} \quad . \tag{s2.4}$$

Here, $C_{\mathrm{IJ}} = C_{\mathrm{I}} + C_{\mathrm{J}}$. Putting Eq.(s1), (s2), and (s3) into Eq.(s4), $\overline{i_{\mathrm{in}}^2}$ is

$$\begin{aligned}\overline{i_{\mathrm{in}}^2} &= \overline{i_{\mathrm{A}}^2} + 4k_{\mathrm{B}}T/R_{\mathrm{F}} + \overline{e_{\mathrm{A}}^2}\left(1/R_{\mathrm{J}}^2 + 1/R_{\mathrm{F}}^2 + (2\pi f)^2 C_{\mathrm{IJ}}^2\right) \\ &\quad + \left(1/R_{\mathrm{J}} + j2\pi f C_{\mathrm{IJ}}\right)\left(\overline{e_{\mathrm{A}} i_{\mathrm{A}}^*} + \overline{e_{\mathrm{A}}^2}\big/R_{\mathrm{F}}\right) + \left(1/R_{\mathrm{J}} - j2\pi f C_{\mathrm{IJ}}\right)\left(\overline{i_{\mathrm{A}} e_{\mathrm{A}}^*} + \overline{e_{\mathrm{A}}^2}\big/R_{\mathrm{F}}\right)\end{aligned} \quad . \tag{s2.5}$$

S2.2 Noises of the proposed CryoSTM-TIA

S2.2.1 The equivalent input noise voltage and the equivalent input noise current of Inv-Amp

For the Inv-Amp, the equivalent input noise voltage and equivalent input noise current of JFET are denoted as e_{J} and i_{J} respectively, and their harmonic components of f is are denoted as E_{J} and I_{J} respectively. g_{m} is the transconductance of JFET and g_{d} is channel conductance of JFET. The noise voltage of the resistors R_{H} is denoted as e_{RH}, and the harmonic components of f are denoted as E_{RH}. The noise voltage of the resistors R_1, R_2, and the feedback resistance R_{f} are denoted as e_{L1}, e_{L2} and e_{f} respectively, and the harmonic components of f are denoted as E_{L1}, E_{L2}, and E_{f} respectively. The noise voltage of the resistors R_{c1} and R_{c2} are denoted as e_1, e_2 and e_{f} respectively, and the

harmonic components of f are denoted as E_1, E_2, and E_f respectively. Here, $R_1 = R_2 = R_L$. All noises of R_H, R_1, R_2, R_{c1}, R_{c2}, and R_f above 1 kHz are thermal noise. $R_d = R_L//(1/g_d)$ and $R_{HL} = R_H//R_L$ are denoted. The equivalent input noise voltage and equivalent input noise current of Rear-OPA are denoted as e_a and i_a respectively, and the harmonic components of f are denoted as E_a and I_a respectively. These noise sources are independent of each other. For the Inv-Amp consistent of the Pre-Amp and Post-Amp, its equivalent input noise voltage and equivalent input noise current as e_A and i_A, the corresponding harmonic components of f are E_A and I_A respectively.

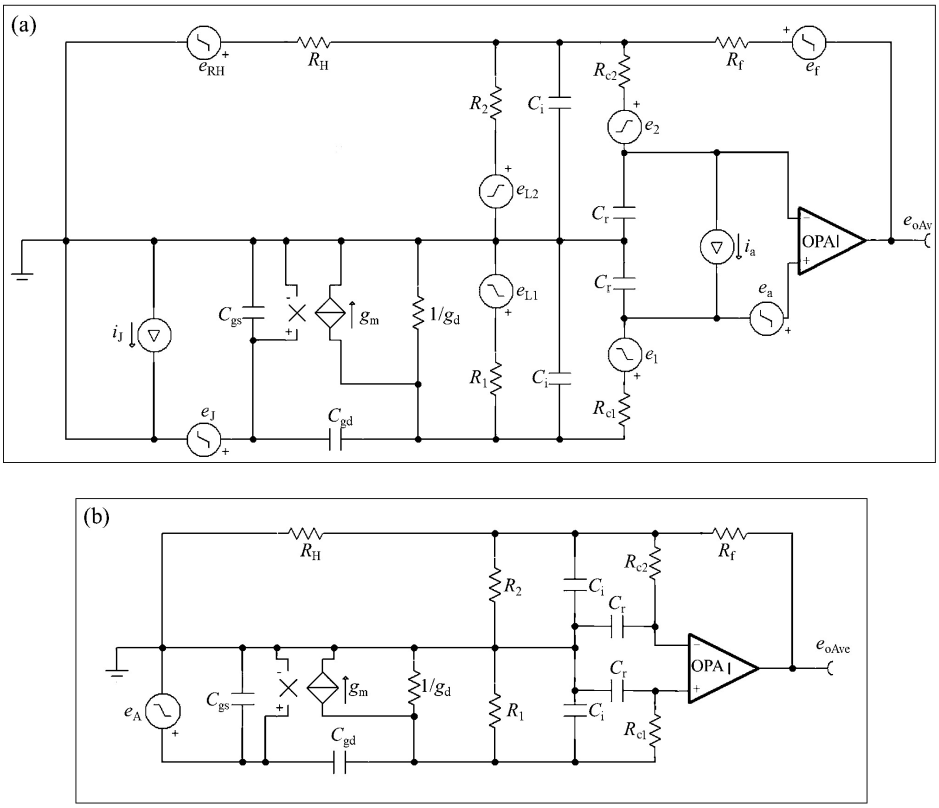

Figure s2.3 (a) Inv-Amp equivalent differential circuit with the input short-circuit containing all noise sources, and the output noise current of e_{oAv}; (b) Noiseless Inv-Amp circuit with the equivalent input noise voltage of the Inv-Amp e_A as the input signal, and the output noise voltage of e_{oAve}; the equivalency of the upper two circuits means $e_{oAv} = e_{oAve}$. In (a) and (b), the triangle OPA is the Rear-OPA.

The equivalent differential circuit of the Inv-Amp containing all noise sources with the input short-circuit is shown as Fig.s2.3(a), and the output noise is e_{oAv}. The noiseless circuit with the equivalent input noise voltage of the Inv-Amp e_A as the input signal is shown as Fig.s2.3(b), and the output noise is e_{oAve}. For calculating the equivalent input

noise voltage of the Inv-Amp, the equations are established on $e_{oAv} = e_{oAve}$. Therefore, by the nodal analysis method,

$E_A \approx E_J + E_{RH}Z_{HL}/(A_{vP1}R_H) - E_{L1}/(g_m R_L) + Z_{HL}(E_{L2}/R_L + E_f/R_f)/A_{vP1}$

$+ E_a/A_{vPj} + (E_1 - E_2)/A_{vP1} - (1/g_m + Z_{HL}/A_{vPj})I_a$,

where $A_{vP1} = g_m/[1/R_d + j(2\pi f)C_i]$, $A_{vPj} = g_m/[1/R_d + j(2\pi f)C_{ir}]$, $Z_{HL} = R_{HL}/[1 + j(2\pi f)R_{HL}C_{ir}]$, $R_d = 1/(1/R_L + g_d)$, and $C_{ir} = C_i + C_r$.

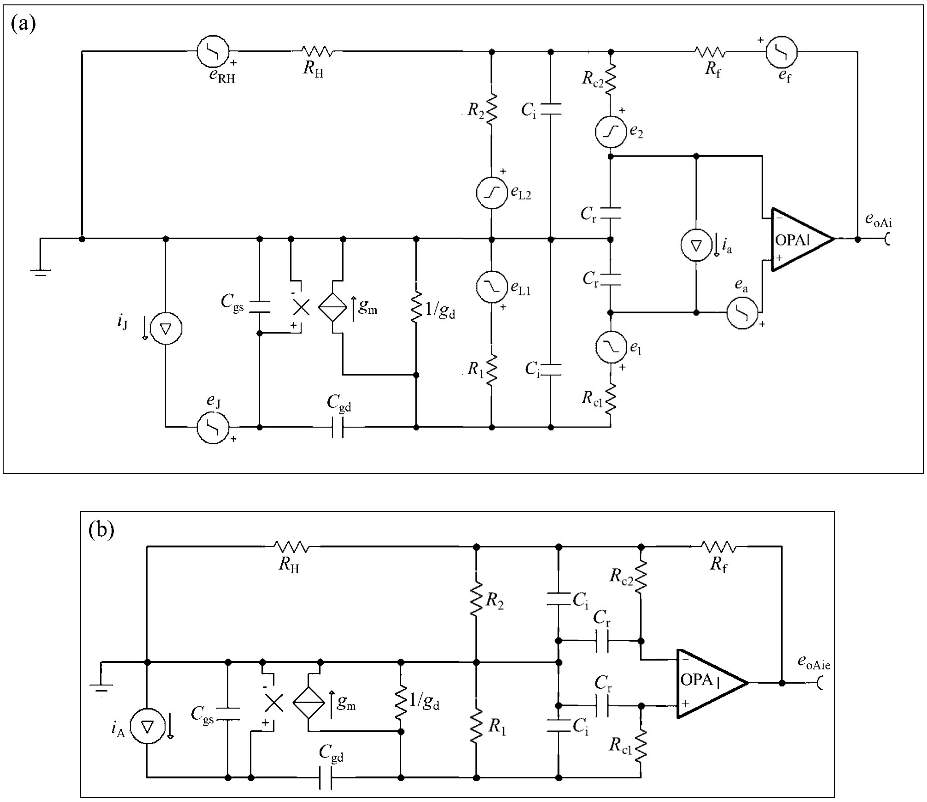

Figure s2.4 (a) Inv-Amp equivalent differential circuit with the input open-circuit containing all noise sources, and the output noise voltage of e_{oAi}; (b) Noiseless Inv-Amp circuit with the equivalent input noise current of the Inv-Amp i_A as the input signal, and the output noise voltage of e_{oAie}; the equivalency of the upper two circuits means $e_{oAi} = e_{oAie}$. In (a) and (b), the triangle OPA is the Rear-OPA.

The equivalent differential circuit of the Inv-Amp containing all noise sources with the input open-circuit is shown as Fig.s2.4(a), and the output noise is e_{oAi}. The noiseless circuit with the equivalent input noise current of the Inv-Amp i_A as the input signal is shown as Fig.s2.4(b), and the output noise is e_{oAie}. For calculating the equivalent input

noise current of the Inv-Amp, the equations are established on $e_{oAi} = e_{oAie}$. Therefore, by the nodal analysis method,

$I_A \approx I_J + j(2\pi f)C_{A1}E_{RH}Z_{HL}/(A_{vP1}R_H) - j(2\pi f)C_{sd}E_{L1}/(g_m R_L) + j(2\pi f)\,(E_1-E_2)/A_{vP1}$

$+ j(2\pi f)C_{A1}Z_{HL}(E_{L2}/R_L+E_f/R_f)/A_{vP1} - j(2\pi f)C_{Aj}E_a/A_{vPj} - j(2\pi f)(C_{sd}/g_m + C_{Aj}Z_{HL}/A_{vPj})I_a$,

where $C_{A1} = C_{gs}+C_{gd}(1+A_{vP1})$, $C_{sd} = C_{gs}+C_{gd}$, and $C_{Aj} = C_{gs}+C_{gd}(1+A_{vPj})$.

For the measured frequency of $f_m < 100$ kHz, $2\pi fC_i < 100$ μS with C_i=160 pF and $2\pi fC_r$ <35 μS with C_r = 50 pF, while $1/R_d$ = 0.55 mS and $1/R_{HL}$ = 0.92 mS, so $A_{vP1} = g_m/[1/R_d+j(2\pi f)C_i]$ and $A_{vPj} = g_m/[1/R_d+j(2\pi f)C_{ir}]$ can be simplified to $-A_{vP} = g_m R_d$, therefore $Z_{HL} \approx R_{HL}$, and $C_{Aj} \approx C_A$. Thus,

$$\begin{pmatrix} E_A \\ I_A \end{pmatrix} = \begin{pmatrix} 0 \\ 1 \end{pmatrix} I_J + \begin{pmatrix} 1 \\ 0 \end{pmatrix} E_J - \begin{pmatrix} 1 \\ j(2\pi f)C_A \end{pmatrix} \frac{R_{HL}E_{RH}}{A_{vP}R_H} - \begin{pmatrix} 1 \\ j(2\pi f)C_{sd} \end{pmatrix} \frac{E_{L1}}{g_m R_L} - \begin{pmatrix} 1 \\ j(2\pi f)C_A \end{pmatrix} \frac{R_{HL}E_{L2}}{A_{vP}R_L}$$
$$- \begin{pmatrix} 1 \\ j(2\pi f)C_A \end{pmatrix} \frac{R_{HL}E_f}{A_{vP}R_f} - \begin{pmatrix} 1 \\ j(2\pi f)C_A \end{pmatrix} \frac{E_1 - E_2 - E_a}{A_{vP}} - \begin{pmatrix} 1 + R_{HL}/R_d \\ j(2\pi f)\left(C_{sd} + C_A R_{HL}/R_d\right) \end{pmatrix} \frac{I_a}{g_m} . \tag{s2.6}$$

Ignoring the small quantities, such as the thermal noise of R_1, R_2, and R_f,

$$\overline{e_A^2} \doteq \overline{e_J^2} + \left[\left(R_{HL}^2/R_H^2\right)\overline{e_{RH}^2} + \left(\overline{e_a^2}+\overline{e_1^2}+\overline{e_2^2}\right)\right]\Big/A_{vP}^2 + \left(1+R_{HL}/R_d\right)^2 \overline{i_a^2}\Big/g_m^2 \quad , \tag{s2.7}$$

$$\overline{i_A^2} \doteq \overline{i_J^2} + (2\pi f)^2 C_A^2 \frac{R_{HL}^2}{R_H^2}\frac{\overline{e_{RH}^2}}{A_{vP}^2} + (2\pi f)^2 C_A^2 \frac{\left(\overline{e_a^2}+\overline{e_1^2}+\overline{e_2^2}\right)}{A_{vP}^2} + (2\pi f)^2 \left(C_{sd} + \frac{R_{HL}}{R_d}C_A\right)^2 \frac{\overline{i_a^2}}{g_m^2} , \tag{s2.8}$$

$$\overline{e_A i_A^*} = \left(\overline{i_A e_A^*}\right)^* \doteq -j(2\pi f)\left[C_A\left(\frac{R_{HL}^2}{R_H^2}\frac{\overline{e_{RH}^2}}{A_{vP}^2} + \frac{\overline{e_a^2}+\overline{e_1^2}+\overline{e_2^2}}{A_{vP}^2}\right) + \left(C_{sd} + \frac{R_{HL}}{R_d}C_A\right)\left(1+\frac{R_{HL}}{R_d}\right)\frac{\overline{i_a^2}}{g_m^2}\right]. \tag{s2.9}$$

Here, $\overline{e_J^2}$ is the equivalent input noise voltage PSD of the JFET and $\overline{i_J^2}$ is their equivalent input noise current PSD. $\overline{e_a^2}$ is the equivalent input noise voltage PSD of the Rear-OPA and $\overline{i_a^2}$ is its equivalent input noise current PSD. $\overline{e_1^2}$ and $\overline{e_2^2}$ are the thermal noise voltage PSD of R_{c1} and R_{c2} respectively.

$\overline{e_1^2} = \overline{e_2^2} = 4k_B T_R R_c = 1.66\ (\mathrm{nV})^2/\mathrm{Hz}$, where T_R is 300 K. $\overline{e_a^2} = 2.25\ (\mathrm{nV})^2/\mathrm{Hz}$ and $\overline{i_a^2} = 4\ (\mathrm{pA})^2/\mathrm{Hz}$ in $f \geq 10$ kHz [S2R4]. In Eq.(s2.7), $\left(1+R_{HL}/R_d\right)^2 \overline{i_a^2}\big/g_m^2$ is one order

of magnitude smaller than $\overline{e_{\mathrm{J}}^2}$. Further ignoring the small quantities in Eq.(s2.7),

$$\overline{e_{\mathrm{A}}^2} \doteq \overline{e_{\mathrm{J}}^2} + \left(\overline{e_{\mathrm{a}}^2} + \overline{e_1^2} + \overline{e_2^2}\right) \Big/ A_{\mathrm{vP}}^2 , \tag{s.10}$$

S4.2.3 The equivalent input noise current of the proposed CryoSTM-TIA

Putting Eq.(s2.8), (s2.9), and (s2.10) into Eq.(s2.5), the equivalent input noise current PSD of the proposed CryoSTM-TIA $\overline{i_{\mathrm{in}}^2}$ is obtained as

$$\begin{aligned} \overline{i_{\mathrm{in}}^2} &= \overline{i_{\mathrm{J}}^2} + 4k_{\mathrm{B}}T/R_{\mathrm{F}} + \left(1/R_{\mathrm{J}} + 1/R_{\mathrm{F}}\right)^2 \left[\overline{e_{\mathrm{J}}^2} + \left(\overline{e_{\mathrm{a}}^2} + \overline{e_1^2} + \overline{e_2^2}\right) \Big/ A_{\mathrm{vP}}^2\right] \\ &+ \left(2\pi f\right)^2 \left[C_{\mathrm{IJ}}^2 \overline{e_{\mathrm{J}}^2} + C^2 \frac{\overline{e_{\mathrm{a}}^2} + \overline{e_1^2} + \overline{e_2^2} + R_{\mathrm{HL}}^2 \overline{e_{\mathrm{RH}}^2} \big/ R_{\mathrm{H}}^2}{A_{\mathrm{vP}}^2} + \left(C_{\mathrm{sdI}} + \frac{R_{\mathrm{HL}}}{R_{\mathrm{d}}} C\right)^2 \frac{\overline{i_{\mathrm{a}}^2}}{g_{\mathrm{m}}^2}\right] , \end{aligned} \tag{s11}$$

where $C_{\mathrm{IJ}} = C_{\mathrm{I}} + C_{\mathrm{J}}$ and $C = C_{\mathrm{A}} + C_{\mathrm{I}} + C_{\mathrm{J}}$ and $C_{\mathrm{sdI}} = C_{\mathrm{gs}} + C_{\mathrm{gd}} + C_{\mathrm{I}} + C_{\mathrm{J}}$. Eq.(s2.11) is Eq.(3.8) in Article.

[S2R1] A. van der Ziel, Noise in Solid State Devices and Circuits, Wiley-Inter-Science, New York, (1986).

[S2R2] Y.X. Liang, Low-noise large-bandwidth transimpedance amplifier for measuring scanning tunneling shot noise spectra in cryogenic STM and its applications, Ultramicroscopy, 234 (2022) 13466.

[S2R3] Z.H. Qian, Study on noise models algorithms and matrix descriptions for integrated circuits, J. Northeast Norm. Univ. 35 (2003) 41.

[S2R4] Data sheet of THS4021 OPA,https://www.ti.com/lit/ds/symlink/ths4021.pdf.3.

Supplemental file3: Equivalent input noise current of JFET

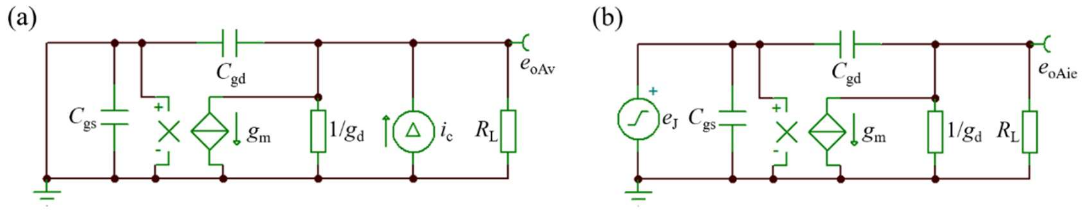

Figure s3.1 (a) JFET equivalent differential circuit with the input short-circuit with i_c, and the output noise voltage of e_{oAv}; (b) Noiseless JFET circuit with its equivalent input noise voltage e_J as the input signal, and the output noise voltage of e_{oAve}; the equivalency of the upper two circuits means $e_{oAv} = e_{oAve}$.

In the equivalent input noise current PSD of Inv-Amp $\overline{i_A^2}$

$$\overline{i_A^2} \doteq \overline{i_J^2} + (2\pi f)^2 C_A^2 \frac{R_{HL}^2}{R_H^2} \frac{\overline{e_{RH}^2}}{A_{vP}^2} + (2\pi f)^2 C_A^2 \frac{\left(\overline{e_a^2} + \overline{e_1^2} + \overline{e_2^2}\right)}{A_{vP}^2} + (2\pi f)^2 \left(C_{sd} + \frac{R_{HL}}{R_d} C_A\right)^2 \frac{\overline{i_a^2}}{g_m^2},$$

$\overline{i_J^2}$ is a major component, but it is very difficult to obtain its value by measurements [S2R1]. $\overline{i_J^2}$ is produced by many noise sources, and the JFET channel noise is one of them. The equivalent differential circuit of the JFET with i_c with the input short-circuit is shown as Fig.s3.1(a), and the output noise is e_{oAv}. The noiseless circuit with the equivalent input noise current of the JFET e_J as the input signal is shown as Fig.s3.1(b), and the output noise is e_{oAve}. For calculating the equivalent input noise voltage of the JFET, the equations are established on $e_{oAv} = e_{oAve}$. Therefore, $\overline{e_J^2} \doteq \overline{i_c^2} / g_m^2$ can be obtained. Assuming i_J is only produced by the JFET channel noise, let us estimate its value. The JFET is at the same operating point for the input open-circuit and the input short-circuit, therefore the JFET channel noise is same. The equivalent differential circuit of the JFET with i_c with the input open-circuit is shown as Fig.s3.2(a), and the output noise is e_{oAi}. The noiseless circuit with the equivalent input noise current of the JFET i_J as the input signal is shown as Fig.s3.2(b), and the output noise is e_{oAie}. For calculating the equivalent input noise current of the JFET, the equations are established

on $e_{oAi} = e_{oAie}$. Solving $e_{oAi} = e_{oAie}$, $\overline{i_J^2} \doteq (2\pi f)^2 C_{sd}^2 \overline{i_c^2} / g_m^2$, where $C_{sd} = C_{gs} + C_{gd}$. Therefore, $\overline{i_J^2} \doteq (2\pi f)^2 C_{sd}^2 \overline{e_J^2}$.

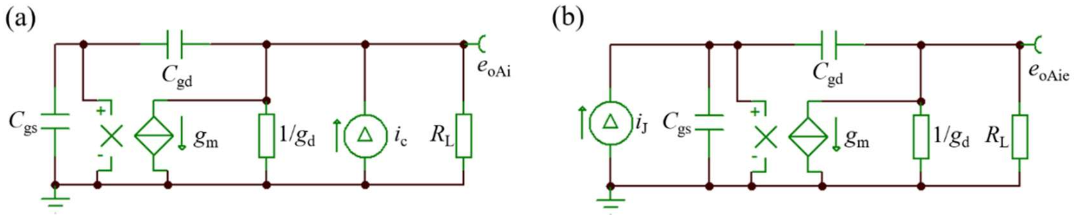

Figure s3.2 (a) JFET equivalent differential circuit with the input open-circuit with i_c, and the output noise voltage of e_{oAi}; (b) Noiseless JFET circuit with its equivalent input noise current i_J as the input signal, and the output noise voltage of e_{oAie}; the equivalency of the upper two circuits means $e_{oAi} = e_{oAie}$.

[S3R1] D. Quan, Y.X. Liang, D. Ferry, A. Cavanna, U. Gennser, L. Couraud, and Y. Jin, Ultra-low noise high electron mobility transistors for high-impedance and low frequency deep cryogenic readout electronics, Appl. Phys. Lett., 105 (2014) 013504 .